New Route to Optical Chaos: Successive-Subharmonic-Oscillation Cascade in a Semiconductor Laser Coupled to an External Cavity

Takaaki Mukai and Kenju Otsuka
Musashino Electrical Communication Laboratories, Nippon Telegraph and Telephone Corporation, Musashino-shi, Tokyo, 180 Japan
(Received 18 March 1985)

Successive-subharmonic-oscillation cascade up to the fifth order followed by chaotic emission (parametric instability) is experimentally observed for the first time in an AlGaAs laser diode coupled to an external cavity. This phenomenon is attributed to the nonlinear interaction between the lasing and amplified-spontaneous-emission modes through the refractive-index dependence on carrier density in the active layer. Observed instabilities are successfully reproduced by the numerical simulations based on the generalized van der Pol equations including the asymmetric intermode interaction.

PACS numbers: 05.40. + j, 42.55.Px

Instability in a laser system was observed clearly for the first time[1] and theoretically verified quite recently[2] by Casperson. In autonomous laser systems, only a few routes to chaotic behavior, such as "period doubling" and "two frequencies" as well as "intermittency," have been demonstrated for the so-called class-C lasers[3] (e.g., far infrared lasers) by several authors.[4–6] These three routes to chaos, which are strongly analogous to the classic routes to chaos studied in fluids, have been recently modeled on the basis of the semiclassical laser (Maxwell-Bloch) equations by Shih, Milonni, and Ackerhalt.[7] It seems likely that the link between fluids and lasers by the Lorenz equations provides reasons for strong similarity.[8] Class-B lasers (e.g., semiconductor, CO_2), where the adiabatic elimination of polarization is valid, have been shown to reach unstable operation only in the presence of external modulation[9] or light injection.[10–14] Recently, brief experimental results suggesting period-three modulation[12,15] and chaotic pulsation[16,17] have been reported in laser diodes (LDs) coupled to an external cavity. However, the bifurcation routes to chaos are still obscure.

This Letter provides the first clear evidence for a new route, that is, a novel "successive subharmonic modulation route," to chaos (parametric instability) in an autonomous laser system, which cannot be explained by the Lorenz model. This evidence is provided through the simultaneous observation of the power spectrum, mode spectrum, and oscillation wave form in a semiconductor laser strongly coupled to an external cavity. The origin of this phenomenon is attributed to the refractive-index dependence on carrier density in the active layer of the LD. Müller and Glas[18] predicted the sequence of pulses with (almost regularly) modulated peaks for a delayed-feedback laser system, on the basis of numerical simulations. However, their model does not include this anomalous dispersion effect and is insufficient for an explanation of our new observations.

Experiments are performed with use of a temperature-stabilized (±0.02 °C) cw AlGaAs CSP laser (length 300 μm) with a gold-coated external mirror, separated by $L_{ext}=39$ cm [inset of Fig. 1]. The oscillation wave form and the power spectrum are observed with an Si avalanche photodiode (APD) followed by a wide-band (~1 GHz) oscilloscope and an rf spectrum analyzer, respectively. A 0.5-m grating monochromator and a temperature-stabilized scanning confocal Fabry-Perot (FP) etalon (free spectral range 3 GHz) are respectively employed to observed the diode cavity mode spectrum and the fine oscillating mode spectrum within a single diode cavity mode.

The light output versus the dc injection current (L-I) relationship for both the solitary LD and the coupled-cavity LD are shown in Fig. 1. The external mirror reduces the threshold current from I_{th0} to I_{th1} and gives rise to a kink in the L-I curve. No modulation is applied plied to the LD.

The fundamental instability, whose frequency f_c is nearly equal to $f_e=c/2L_{ext}\cong 380$ MHz (c is the velocity of light), is observed at a bias below the kink. The power spectrum, the mode spectrum, and the oscillating wave form are shown in Figs. 2(a), 3(a), and 3(a′), respectively.

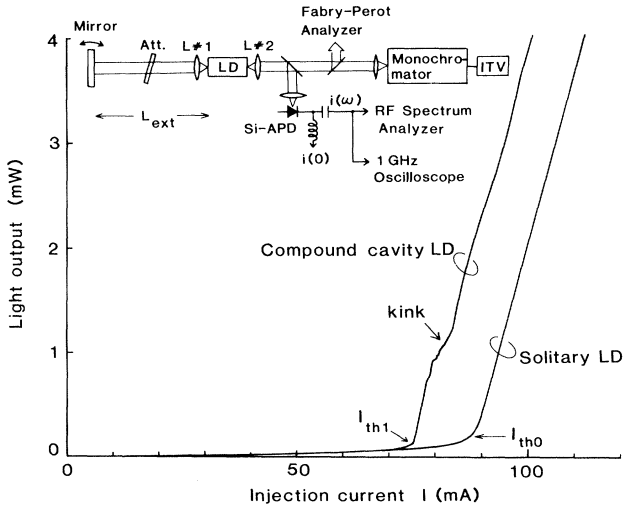

FIG. 1. Light output vs dc injection current curves with and without the external cavity.

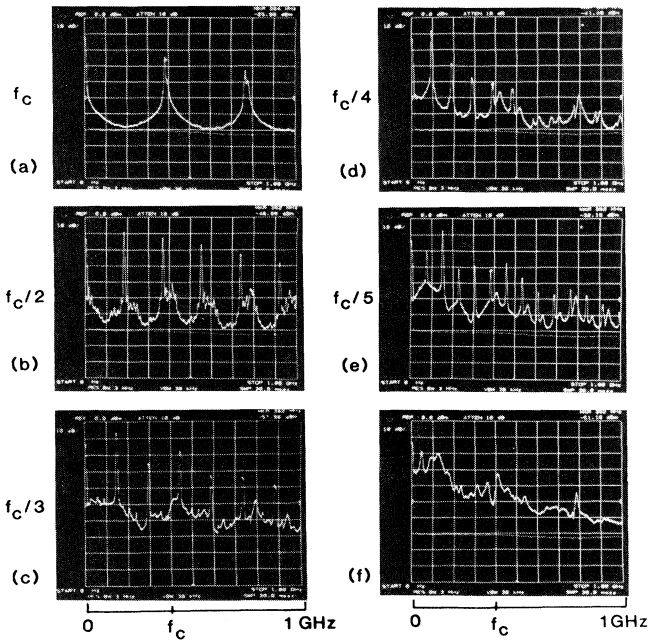

FIG. 2. Observed power spectra of compound cavity LD outputs with (upper traces) and without (lower, faint traces) the external cavity. Vertical: 10 dB/div, horizontal: 100 MHz/div.

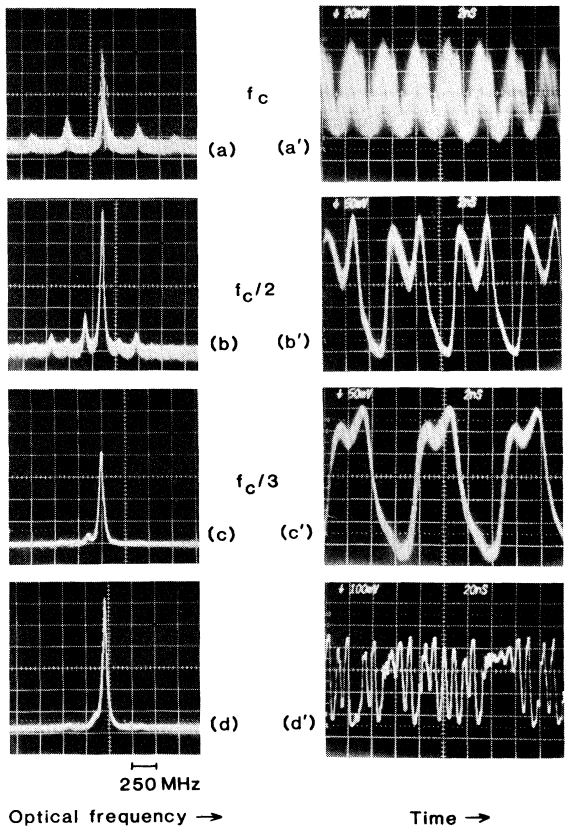

FIG. 3. Observed oscillating mode spectra measured with a FP analyzer (horizontal: 250 MHz/div) and real-time wave forms of compound LD outputs, showing subharmonic cascades to chaos. (a),(a') Fundamental oscillation f_c [(a') scales are 20 mV/div and 2 ns/div]. (b),(b') Subharmonic oscillations $f_c/2$ [(b') scales are 50 mV/div and 2 ns/div], and (c), (c') $f_c/3$ [(c') scales are 50 mV/div and 2 ns/div]. (d),(d') Chaotic pulsation [(d') scales are 100 mV/div and 20 ns/div)]. [(a'), (b'), (c'): synchroscanned wave forms; (d'), single-shot wave form.]

As the injection current is increased into the kink region, and simultaneously the optical feedback is precisely aligned by tilting of the external mirror, successive subharmonic oscillations up to the fifth subharmonic of the fundamental oscillation take place. The observed power spectra corresponding to f_c/m ($m=2,3,4,5$) subharmonic oscillations are shown in Figs. 2(b)—2(e). The line spectral components appearing at f_c/m frequencies are an indication of the real oscillation (not noise) at the subharmonic frequency. This is also confirmed from the FP analyzer mode spectra shown in Figs. 3(b) and 3(c). It is worthwhile mentioning that the subharmonic oscillating mode power in the lower-frequency side is larger than that in the higher-frequency side, as is clearly seen in Fig. 3(b). The real-time wave forms reveal that the compound cavity LD outputs are modulated with subharmonic periods $T_m=m/f_c$ [Figs. 3(b') and 3(c')].

As the injection current is increased toward the edge of the kink region, the subharmonic oscillations break into chaotic pulsations, as shown in Fig. 3(d'). In the chaotic regime, the broad-band noise has filled the spectrum between the originally separated peaks [Fig. 2(f)], which is reflected in the broadened spectral width in the mode spectrum [Fig. 3(d)].

When the subharmonic oscillations and chaotic emissions are clearly observed, the LD shows single or multiple compound-cavity—mode oscillations within a single longitudinal diode cavity resonance mode. As the injection current is increased beyond the kink region, the compound-cavity LD breaks into multi-longitudinal-mode oscillations which spread over several diode cavity resonance modes. In this case, no line spectral component is observed. Noise-spectrum broadening at f_c and its harmonics is enhanced by an increase in the injection current.

The successive subharmonic oscillations demonstrated here are different from those in Ref. 15, where the power spectrum suggesting the third subharmonic modulation of the relaxation oscillation at a frequency different from f_e was observed at far above the threshold ($\sim 1.6 I_{\rm th}$) for an LD weakly coupled to an external cavity. The present oscillatory instability is clearly observed only below the original threshold $I_{\rm th0}$ for the solidary LD. This means that the presence of the external mirror does not act just as a perturbation to the solitary LD, but the entire system is considered to be completely autonomous in the present

operating regime.

Turning our attention to the fundamental physical process responsible for the observed instabilities, we find that the spontaneously emitted photons coupled into the active wave guide are amplified by traveling back and forth between the end facets. In the case of a solitary LD, these amplified spontaneous emissions (ASEs), having wide spectral components over 10 to 30 nm, are enhanced at the diode cavity resonance frequencies separated from each other by about 120 GHz. Each of these diode cavity modes has a full-gain bandwidth of several gigahertz at half maximum (FWHM).[19]

The effective reflectivity of our external mirror is estimated to be 0.2 from the reduction in threshold currents, which yields a finesse of 4 for the external cavity. This frequency-dependent optical feedback enhances the ASE components at the frequencies separated by the inverse round-trip time, that is, $f_e \cong 380$ MHz. These ASE resonance mode frequencies, which are indicated by the open circles on the abscissa in Fig. 4, are determined only by the external cavity length L_{ext} and are insensitive to the feedback condition.

On the other hand, the eigenfrequencies of the compound-cavity lasing modes are determined from the phase continuum condition[20,21] given by the equations indicated in Fig. 4. These frequencies are given by the intersections (solid circles) of these two curves and are sensitively changed by the phase shift introduced here by the mirror tilt. As a consequence, the frequency separation between the ASE and lasing modes can be easily changed by adjustment of the external mirror.

The observed instability can be interpreted in terms of the parametric interaction of these ASE and compound-cavity lasing modes stemming from the refractive-index dependence on carrier density in the active layer of an LD, which is characterized by the so-called α parameter. According to the analysis by Bogatov, Eliseev, and Sverdlov,[22] if a probe beam E_a (ASE mode) at frequency ω_a is introduced into the gain medium, which is saturated by the laser radiation E_s (compound cavity lasing mode) at frequency ω_s, the carrier density is modulated by the difference frequency $\Delta\omega = \omega_a - \omega_s$. The temporal variation of the refractive index associated with the carrier-density modulation causes stimulated dynamic scattering of the saturating beam. The amount of scattering is proportional to $E_a E_s E_s^*$. That part of the scattered radiation having the same frequency as that of the probe beam adds constructively to the probe beam, producing a more pronounced amplification when $\omega_a < \omega_s$. On the other hand, the probe-beam amplification is suppressed when $\omega_a > \omega_s$. As a consequence, the ASE at the lower-frequency side obtains an additional gain and breaks into oscillation. Such asymmetric interaction firmly supports the observed oscillating mode spectra shown in Figs. 3(a)–3(d).

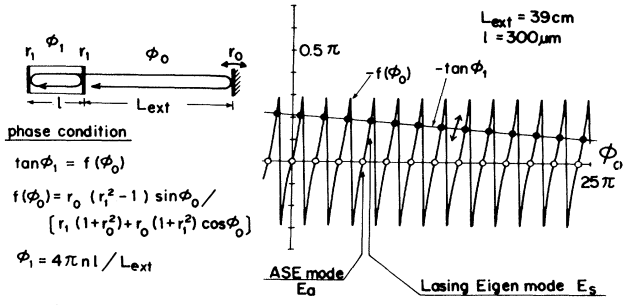

FIG. 4. Frequency arrangement of ASE modes E_a and lasing eigenmodes E_s for a semiconductor laser diode coupled to the external cavity.

The origin of the successive subharmonic oscillations can be understood in physical terms as follows. When the effective detuning frequency between the ASE mode and its neighboring lasing modes, which can be changed by adjusting the external mirror, coincides with a fraction of the inverse round-trip time, the three adjacent modes are resonantly enhanced by the combination-tone polarizations resulting from the aforementioned third-order nonlinear process. As a result, the LD exhibits the subharmonic modulation phenomena. While the detuning frequency is slightly different from the inverse round-trip time, low-frequency components appear and intermittent optical turbulences are thought to arise.

In order to verify the proposed physical mechanism, numerical simulations are carried out based on the generalized van der Pol equations,[10] including the anomalous dispersion effect through the parameter $\alpha = 2(\partial\omega/\partial N)(\partial G/\partial N)^{-1}$ (N is the carrier density, G the gain factor).[12,23] Calculations are carried out assuming three modes, namely, the ASE mode (amplitude E_a at frequency ω_a), and adjacent oscillating compound-cavity mode No. 1 (E_{s1} at ω_{s1}) and No. 2 (E_{s2} at ω_{s2}), as are shown in the inset of Fig. 5, where the detuning, $\omega_a - \omega_{s1}(N_{\text{th}})$, is changed at a constant frequency separation between the two lasing modes, $\omega_{s1}(N_{\text{th}}) - \omega_{s2}(N_{\text{th}})$. The adopted parameter values are $w = P/P_{\text{th}} = 1.25$, $n_e = 1.25$, $q(\tau_{p,s}/P_{\text{th}})^{1/2} = 0.01$, $\alpha = 2$, $\beta = 10^{-5}$, $\tau_{p,a} = 0.2\tau_{p,s}$, and $\tau/\tau_{p,a} = 10^3$, where the same notations used in Ref. 12 are employed.[24]

Figures 5(a)–5(d) show the simulated output wave forms and corresponding power spectra for different detunings. It is apparent from these figures that the successive-subharmonic cascade to deterministic instability can be thoroughly reproduced theoretically by a change in the effective detuning. This more than adequately explains the experimental observations. Furthermore, note that these parametric instabilities completely disappear in the case of $\alpha = 0$.

In conclusion, novel deterministic instability which obeys the subharmonic-oscillation cascade route to chaos has been observed for the first time in a laser diode coupled to an external cavity. The fundamental physical process, that is, the parametric intermode interaction stem-

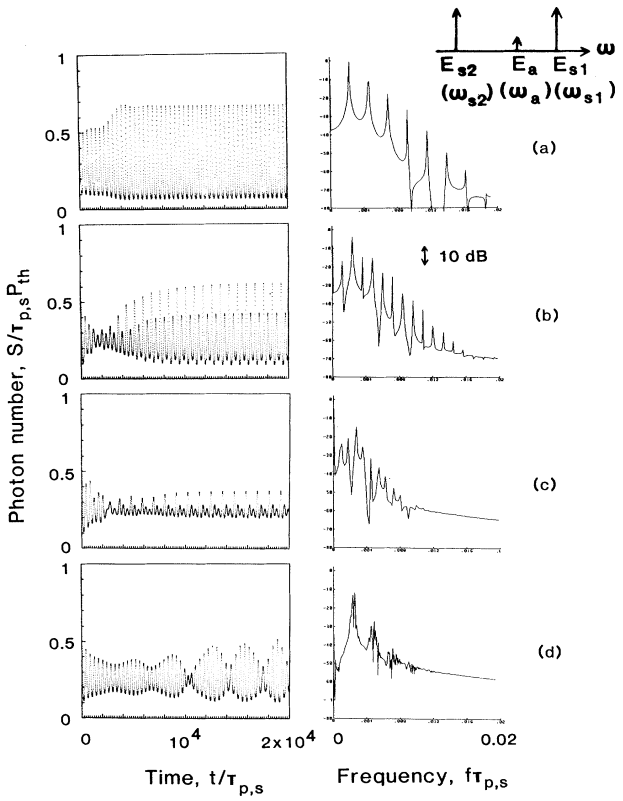

FIG. 5. Simulated output wave forms and corresponding power spectra for different detunings $\Delta_l=(n_e/n)\times[\omega_a-\omega_{sl}(N_{\rm th})](l=1,2)$, where $|\Delta_1|+|\Delta_2|=0.0178$ is fixed. Adopted parameter values are given in the text. (a) $\Delta_1=-0.0172$ (f_c modulation), (b) $\Delta_1=-0.0089$ ($f_c/2$ modulation), (c) $\Delta_1=-0.0071$ ($f_c/3$ modulation), and (d) $\Delta_1=-0.0159$, $q(\tau_{p,s}/P_{\rm th})^{1/2}=0.002$ (intermittency).

ming from the refractive-index dependence on carrier density, has been confirmed by numerical simulation based on the generalized van der Pol equations including the anomalous dispersion effect of the LD. To the best of our knowledge, this is the first clear evidence of optical chaos in autonomous class-B laser systems. From the theoretical point of view, the observed parametric instabilities are not restricted to laser diodes, but they should be expected in other lasers where the lasing frequency is detuned from the gain spectrum peak, i.e., $\alpha\neq 0$.

The authors wish to thank Dr. Hiroshi Kanbe and Dr. Ken'ichi Kubodera for their helpful discussions.

[1]L. W. Casperson, IEEE J. Quantum Electron. **14**, 756 (1978).

[2]L. W. Casperson, J. Opt. Soc. Am. B **2**, 62 (1985).

[3]J. R. Tredicce, F. T. Arecchi, G. L. Lippi, and G. P. Puccioni, J. Opt. Soc. Am. B **2**, 173 (1985).

[4]C. O. Weiss, A. Godone, and A. Olafsson, Phys. Rev. A **28**, 892 (1983).

[5]R. S. Gioggia and N. B. Abraham, Phys. Rev. Lett. **51**, 650 (1983).

[6]See special issue on "Instabilities in active optical media," J. Opt. Soc. Am. B **2** (1985).

[7]M. Shih, P. W. Milonni, and R. Ackerhalt, J. Opt. Soc. Am. B **2**, 130 (1985).

[8]H. Haken, Phys. Lett. **53A**, 77 (1975).

[9]F. T. Arecchi, R. Meucci, G. P. Puccioni, and J. R. Tredicce, Phys. Rev. Lett. **49**, 1217 (1982).

[10]K. Otsuka and H. Iwamura, Phys. Rev. A. **28**, 3152 (1983).

[11]K. Otsuka and H. Kawaguchi, Phys. Rev. A **29**, 2953 (1984).

[12]K. Otsuka and H. Kawaguchi, Phys. Rev. A **30**, 1575 (1984).

[13]K. Otsuka, J. Opt. Soc. Am. B **2**, 168 (1985).

[14]L. A. Lugiato, in Proceedings of the Workshop on Chaotic and Pulse Instabilities, Schloss Elmau, Federal Republic of Germany, May 1984 (unpublished).

[15]H. Kawaguchi and K. Otsuka, Appl. Phys. Lett. **45**, 934 (1984).

[16]P. Glas, R. Müller, and A. Klehr, Opt. Commun. **47**, 297 (1983).

[17]Y. Cho and T. Umeda, J. Opt. Soc. Am. B **1**, No. 3 (1984).

[18]R. Müller and P. Glas, J. Opt. Soc. Am. B **2**, 184 (1985).

[19]T. Mukai and Y. Yamamoto, IEEE J. Quantum Electron. **17**, 1028 (1981).

[20]A. Olsson and C. L. Tang, IEEE J. Quantum Electron. **17**, 1320 (1981).

[21]T. Fujita, S. Ishizuka, K. Fujito, H. Serizawa, and H. Sato, IEEE J. Quantum Electron. **20**, 492 (1984).

[22]A. P. Bogatov, P. G. Eliseev, and B. N. Sverdlov, IEEE J. Quantum Electron. **11**, 510 (1975).

[23]R. Lang and K. Kobayashi, IEEE J. Quantum Electron. **16**, 347 (1980).

[24]P is the pumping rate, $n_e=n+\Omega(\partial n/\partial\Omega)$ is the effective refractive index, Ω is the oscillation frequency, q is the coupling coefficient, β is the spontaneous emission coefficient, $\tau_{p,a}$ and $\tau_{p,s}$ are the photon lifetimes for the ASE mode and oscillating compound-cavity modes, respectively, and τ is the carrier lifetime. The subscript th denotes the value at the threshold for the compound cavity mode oscillation.

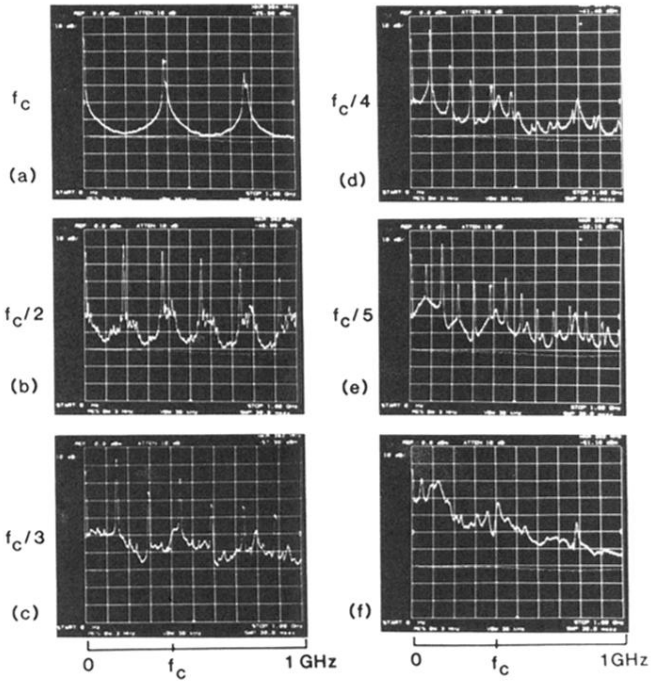

FIG. 2. Observed power spectra of compound cavity LD outputs with (upper traces) and without (lower, faint traces) the external cavity. Vertical: 10 dB/div, horizontal: 100 MHz/div.

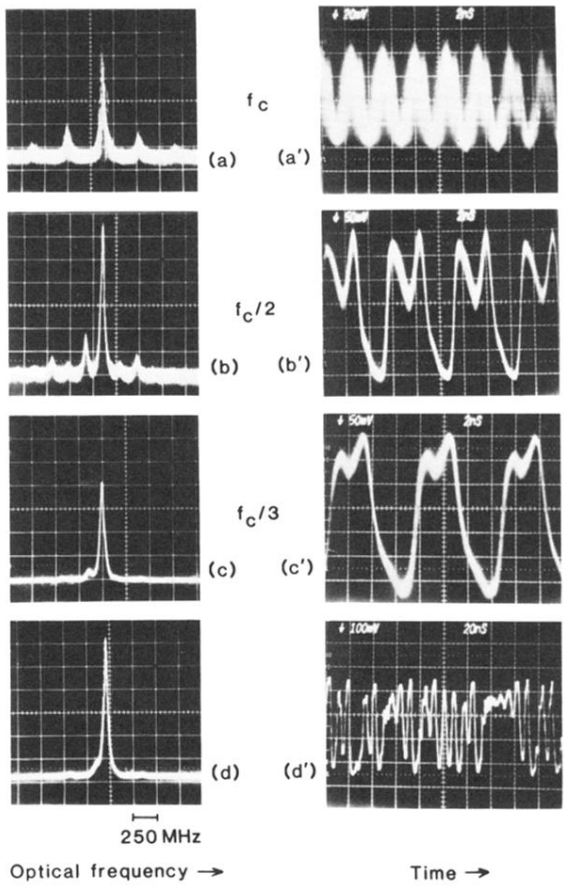

FIG. 3. Observed oscillating mode spectra measured with a FP analyzer (horizontal: 250 MHz/div) and real-time wave forms of compound LD outputs, showing subharmonic cascades to chaos. (a),(a′) Fundamental oscillation f_c [(a′) scales are 20 mV/div and 2 ns/div]. (b),(b′) Subharmonic oscillations $f_c/2$ [(b′) scales are 50 mV/div and 2 ns/div], and (c), (c′) $f_c/3$ [(c′) scales are 50 mV/div and 2 ns/div]. (d),(d′) Chaotic pulsation [(d′) scales are 100 mV/div and 20 ns/div)]. [(a′), (b′), (c′): synchroscanned wave forms; (d′), single-shot wave form.]